Determination of parton density functions from $p\bar{p}$-collsions at $\sqrt{s}$=1.8 TeV and $\sqrt{s}$=0.63 TeV

Federico von Samson-Himmelstjerna

19.9.2007

Abstract: This work treats the implementation and fitting of data for Drell-Yan processes and prompt-photon-production taken at DØ and CDF at Tevatron, Fermilab.
The data and cuts for the Drell-Yan process were taken from [1] and [2]. The ones for prompt-photon-production in [3], [4] and [5] .
The data were implemented as HzTool-routines and the respective Monte Carlo simulation carried out with the PYTHIA event generator.
It appeared that in the case of the Drell-Yan processes using only first order processes (which means here production of Z^0 without jet) leads to a considerably better match of MC- and detector data. But this procedure needs the use of a k-factor. Nontheless these first order processes were used for the fitting.
While the results gained from [5] look promising there were, especially in the comparison with CTEQ61 PDFs, discrepancies observable whose origin needs to be investigated in more detail.

1 Introduction

In the naive parton-model the proton consists only of noninteracting quarks and each quark carries a fraction x of the protons total momentum. This model had to be extended into the so called improved parton model, where the interaction of the quarks, mediated by gluons, is taken into account. The quarks together with the glouns are then called partons. The parton density function (PDF) $f_i(x, Q^2)$ gives then the number of partons of flavor i and charge e_i with the fraction of total momentum x measured at an energyscale Q^2.
In a collision the partons - rather than the entire proton - will interact. By this means it seems reasonable that the measured cross section depends on the PDF of the proton.

$$\frac{d^2\sigma}{dxdQ^2} \propto \sum_i e_i^2 f_i(x, Q^2)x \tag{1}$$

The gluon density function can be approximated by:

$$xg(x) = N(\frac{1}{x})^\alpha (1-x)^\beta \tag{2}$$

here N is a normalizing factor which can be fitted together with α and β. When x is small - which will be the case in the following discussions - $g(x)$ is dominated by $(\frac{1}{x})^\alpha$ and it is sufficient to fit α and N.

This work treats data measured at the Tevatron, Fermilab. The Tevatron is a $p\bar{p}$ collider and the data were taken at center of mass energies of 630 GeV ([4], part 1 of [5]) and 1800 GeV ([1],[2], [3], part 2 of [5]). There were two processes investigated:

1.1 Drell-Yan process ([1],[2])

Drell-Yan processes are characterized by $q\bar{q} \to Z^0 \to f\bar{f}$.

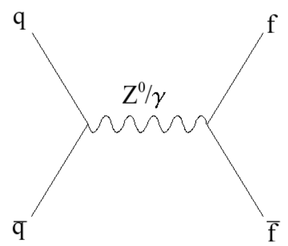

In this case the investigated process is $q\bar{q} \to e^-e^+$. The measured cross section is here $\frac{d\sigma}{dp_T}$. Here p_T stands for the transverse momentum of the Z^0 which corresponds to the net p_T of the e^-e^+-pair.
As $p\bar{p}$ are collinear the net transverse momentum of the system must - due to conservation of momentum - be zero. So if one assumes only a process of the form:

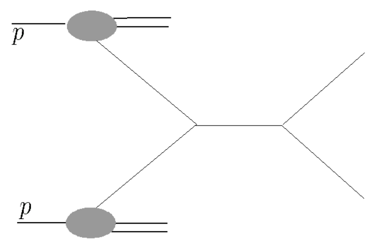

the Z^0 cannot have any transverse momentum at all. Measurement shows that this is not the case.
The reason for the nonvanishing p_T can be found in gluonradiation or more exactly by the fact that the interacting partons can radiate gluons in the initial state. These gluons can carry transverse momentum and by that "allow" the Z^0 to carry a nonvanishing p_T itself. So the above proposed process must be extended e.g like this (the gluon radiation is important not the specific partons wich are interacting). One could also have gluons which radiate further gluons and at the end split into $q\bar{q}$. By that one is also sensitive to the gluon density.

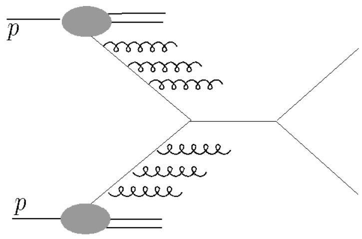

1.2 Prompt-photon production([3],[4],[5])

Prompt-photon productions are characterized by $qg \rightarrow q\gamma$.

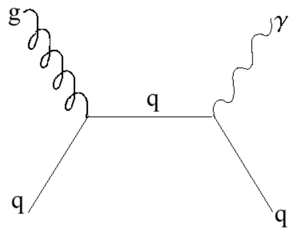

The measured cross sections are here $\frac{d^2\sigma}{dp_t d\eta}$ ([5]) or $\frac{d^2\sigma}{dE_t d\eta}$ ([3], [4]). Where η is the pseudorapidity, p_T the transverse momentum and E_T the transverse energy of the final state photon. E_T is hereby defined as $E_T = E_{tot} sin(\theta)$.
The prompt-photon process can even be seen as a first order correction of the Drell-Yan process as can be seen by turning the above shown Feynman graph about 45°.

1.3 Scanning and Fitting

Fitting parameters of the PDF involves long calculations, because all parameters are changed simultanously. And to obtain good statistics, for each set of parameters a complete event generation with a large number of events has to be constructed.
To get a first insight into the behavior of the parameters one can apply a much quicker scan rather than the long fit. This means that the parameters are changed one after another which reduces the number of full event generations - and so the runtime - remarkably.
At the stage of writing this report only first scanning results can be presented due to the long duration of the calculations.

2 Implementaion of data and event generation

The data were implemented as the following HzTool routines.

reference	HzTool routine	detector	process
[1]	PRL84_5_31012000.F	DØ	Drell-Yan
[2]	PRD61_032004.F	DØ	Drell-Yan
[3]	PRL84_13_27032000.F	CDF	prompt-photon
[4]	PRL87_25_17122001.F	DØ	prompt-photon
[5]	PRD65_112003.F	DØ	prompt-photon

The routines then create histograms of the detector data as well as of normalized MC data. The applied cuts and normalization of the routines are the following:
[1]: $E_T \geq 20$GeV and $\eta < 1.1$ or $E_T \leq 15$GeV and $1.1 < \eta < 4.2$, normalized to luminosity
[2]: $E_T \geq 25$GeV and $\eta < 1.1$ or $1.5 < \eta < 2.5$, normalized to luminosity
[3]: $E_T \geq 10$GeV and $\eta < 0.9$ or $1.6 < \eta < 2.5$, normalized to luminosity and η =1.8
[4]: $E_T \geq 7.5$GeV and $\eta < 0.9$ or $1.6 < \eta < 2.5$, normalized to luminosity and η =1.8
[5]: $E_T \geq 6$GeV and $\eta < 0.9$ ($\sqrt{s} = 630$ GeV) \ $\eta < 0.9$ ($\sqrt{s} = 1800$ GeV), normalized to luminosity and η =1.8

3 Results

The follwing results were obtained using PYTHIA as event generator generating 10^6 events.

3.1 Drell-Yan ([1],[2])

The standard PDF used to obtain the non-fitted data was CTEQ 6.1
before scanning: For both two final states of different order were produced. The first included Z^0 only while the other included $Z^0 + jet$.
The Z^0-only MC data show a good agreement of the shape but were quantitatively too low. This made a multiplication of the data with a k-factor of 2 ([1]) and 3 ([2]) necessary to obtain a quantitative fit of MC- and detector data.
Nevertheless the agreement is worse the lower p_T is (see Fig.1).

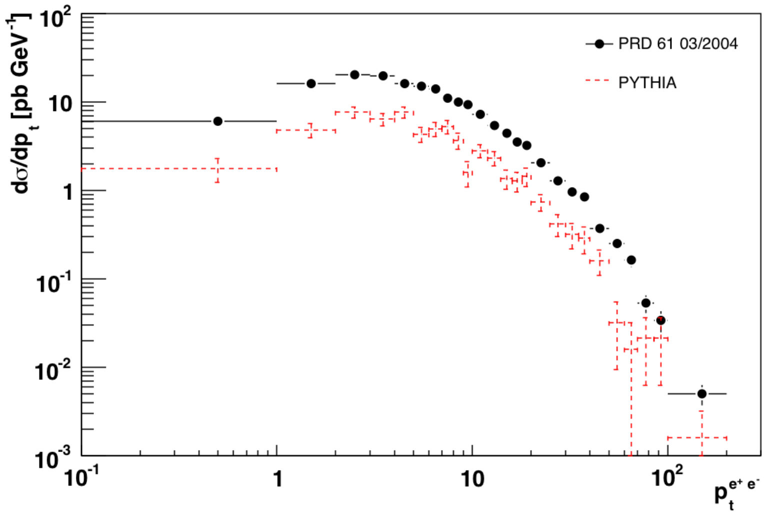

Figure 1: MC data of [2] at 1800 GeV, $\eta < 1.1$ or $1.5 < \eta < 2.5$,using non fitted standard PDF and Z^0-only event selection

The event selection $Z^0 + jet$ gave a better quantitative but a worse qualitative agreement than the Z^0-only data (see Fig.2).

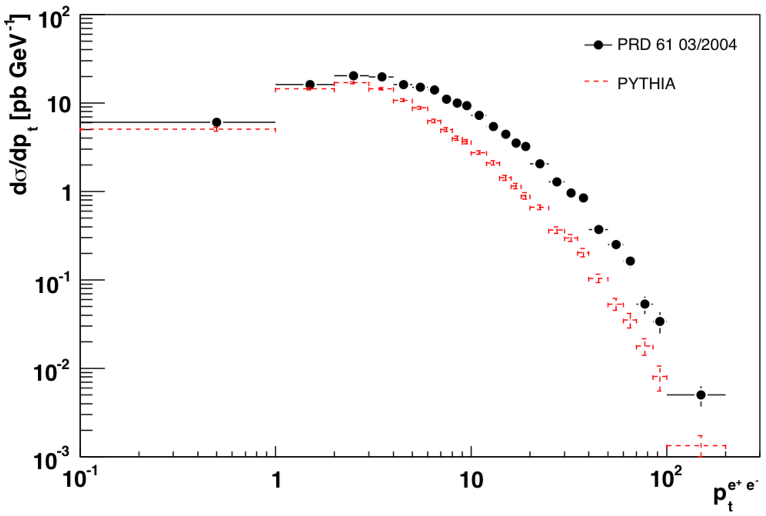

Figure 2: MC data of [2] at 1800 GeV, $\eta < 1.1$ or $1.5 < \eta < 2.5$, using non fitted standard PDF and $Z^0 + jet$ event selection

I decided to use the Z^0-only final state for the scanning.

after scanning: In a first step the only the leading term of the gluon density was scanned, which means scanning N and α in (2). In a second step the quark density was scanned as well. As one can clearly see the quantitative mismatch of MC- and detector-data was corrected by the scanning and no k-factor was needed.
But again one can observe a worse agreement of the data in the low p_T region.

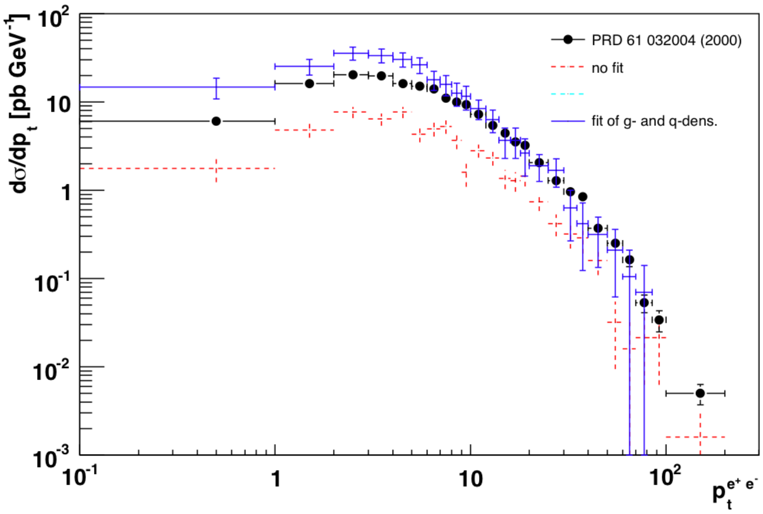

Figure 3: MC data of [2] at 1800 GeV, $\eta < 1.1$ or $1.5 < \eta < 2.5$, after (solid) and before (dashed) scanning and $Z^0 + jet$ event selection

The plots of [1] can be found in the appendix.

3.2 Prompt photon production ([3],[4],[5])

Even before scanning there was already a good agreement of MC- and detector data and the scanning gave a slight improvement of this agreement.
The data of [5] are not well in the low p_T-region. The large errorbars in the high p_T region is due to low statistics in this region (see Fig. 4). Investigating the data of [3] and [4] one observes that the description at low p_T is bad again. Furthermore the $1.6 < \eta < 2.5$ data seem to be systematically to low, while the $\eta < 0.9$ data do not show such systematic tendencies but seem to have a slightly better data match. The plots of [3] and [4] can be found in the appendix. A very strange fact in case of [4] is that the matching of the data got worse after the fitting. This definitely makes a doublecheck of the routines as well as the generator tuning necessary.

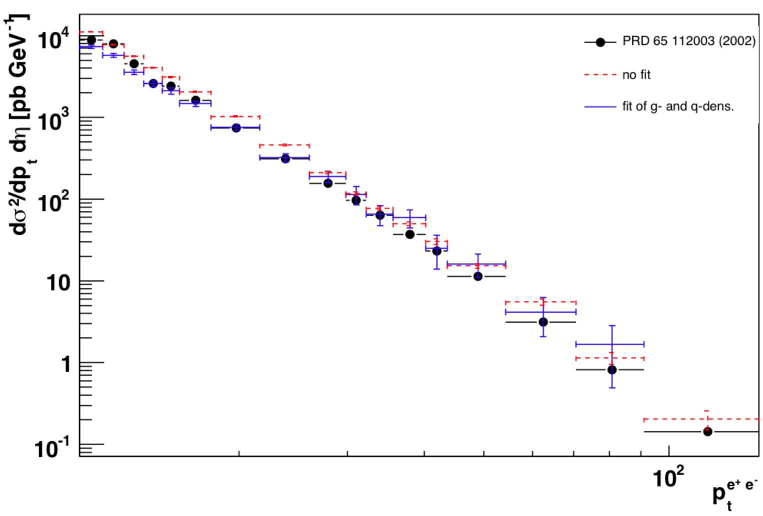

Figure 4: MC data of [5] at 1800 GeV,$\eta < 0.9$, after (solid) and before (dashed) scanning

3.3 Comparison with CTEQ61 results

Out of the scanning results of [2] and [5] plots of gluons and quark densities with respect to x at different Q^2 were made and compared with PDFs given by CTEQ61. The PDF obtained from [5] show at least a similar shape, whereas in case of [2] there is a drastic difference between the two PDFs. Only the valence quark density is unaffected.
These very astonishing and unlikely results demand further investigation.
The graphs can be found in the appendix.

4 Conclusion

The observed mismatch in the low p_T region might be explained by the intrinsic transverse momentum of the partons inside the proton, which might not be neglegible in this p_T region.
There is a good agreement of MC- and detector data which is a result of the scanning procedure. Performing a proper fitting might make this agreement even better.
Although is seems necessary to treat especially the results of [4] with care and the comparison of the fitted PDF with the CTEQ61 PDF shows that - at least in case of [2] - the fit of quark densities do at low x not coincide at all with the one given by CTEQ61. A further investigation and double checking of the routines , tuning and the approach is here definitely necessary.

5 Acknowledgement

At very first I want to thank Antonia. You were my sunshine in these rainy days!
Then I definitely want to thank my supervisor Dr. Hannes Jung and Dipl. Phys. Axel Cholewa for their fantastic support. Thank you for your patience to answer all my questions and for everything you taught me. A big thanks goes as well to Lluis, Tobias, Zlatka, Michael and Krzysztof for the great spirit and atmosphere I found in your group.
I want as well to thank Prof. Dr. Joachim Mayer for making it possible to be part of this group and the DESY for making such an experience possible.

References

[1] T. Affolder *et al.*, Phys. Rev. Lett. 84, 5 (2000).

[2] B. Abbott *et al.*, Phys. Rev. D 61, 032004 (2000).

[3] B. Abbott *et al.*, Phys .Rev. Lett. 84, 13 (2000).

[4] V. M. Abazov *et al.*, Phys. Rev. Lett. 87, 25 (2001).

[5] D. Acosta *et al.*, Phys. Rev. D 65, 112003 (2002).

[6] F. Halzen,A.D. Martin, *Quarks and Leptons, An Introductory Course in Modern Particle Physics*, John Wiley&Sons, 1984

A Graphs

A.1 Drell-Yan

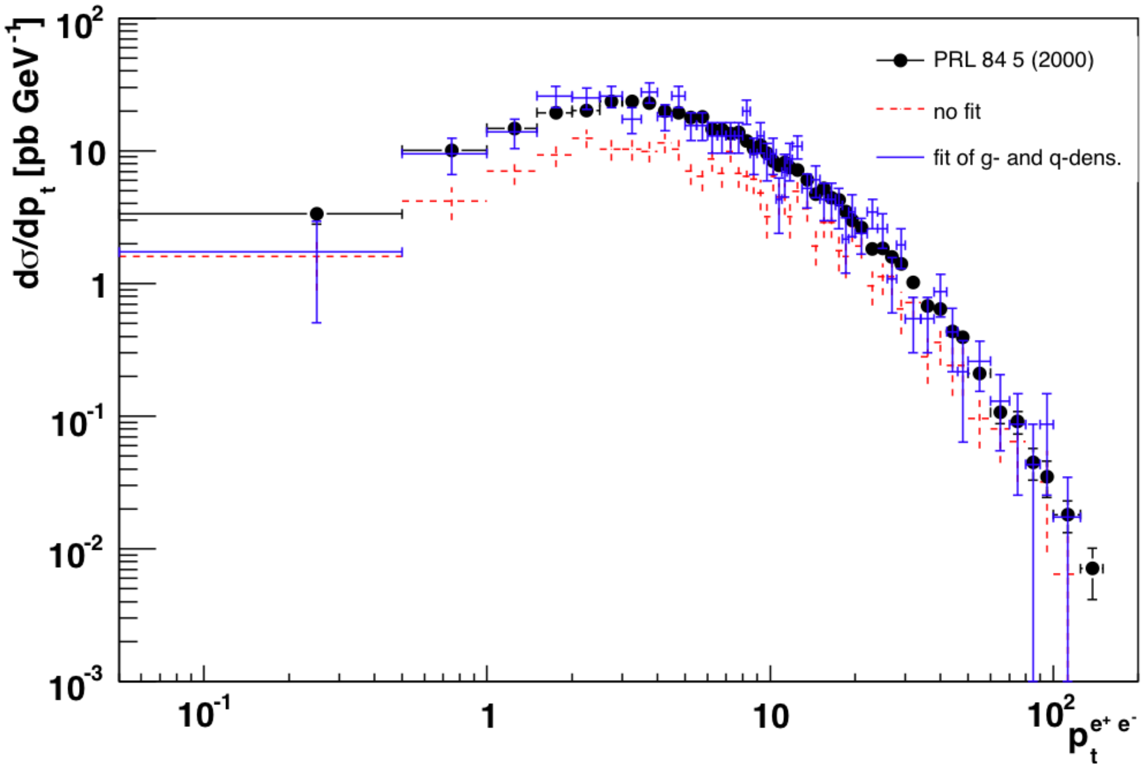

Figure 5: MC data of [1] at $\sqrt{s}$=1800 GeV, $\eta < 1.1$ or $1.1 < \eta < 4.2$, after (solid) and before (dashed) scanning, $Z^0 + jet$ event selection

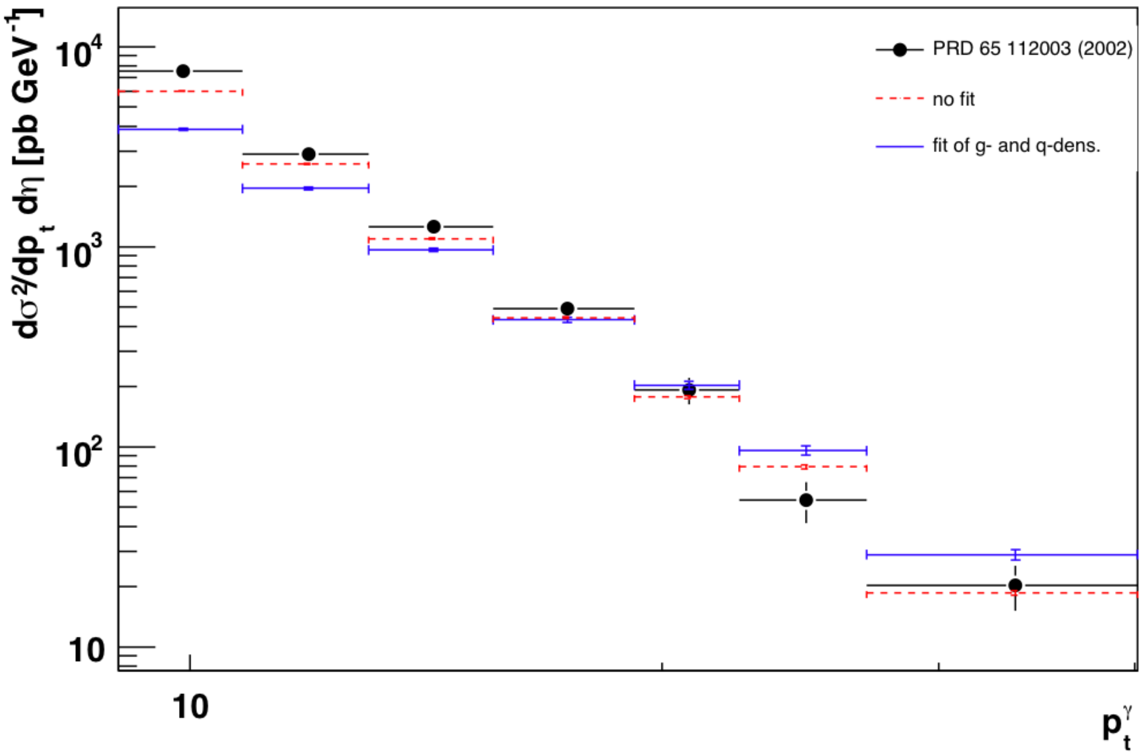

Figure 6: MC data of [5] at $\sqrt{s}$=630 GeV, $\eta < 0.9$,after (solid) and before (dashed) scanning

A.2 Prompt-photon

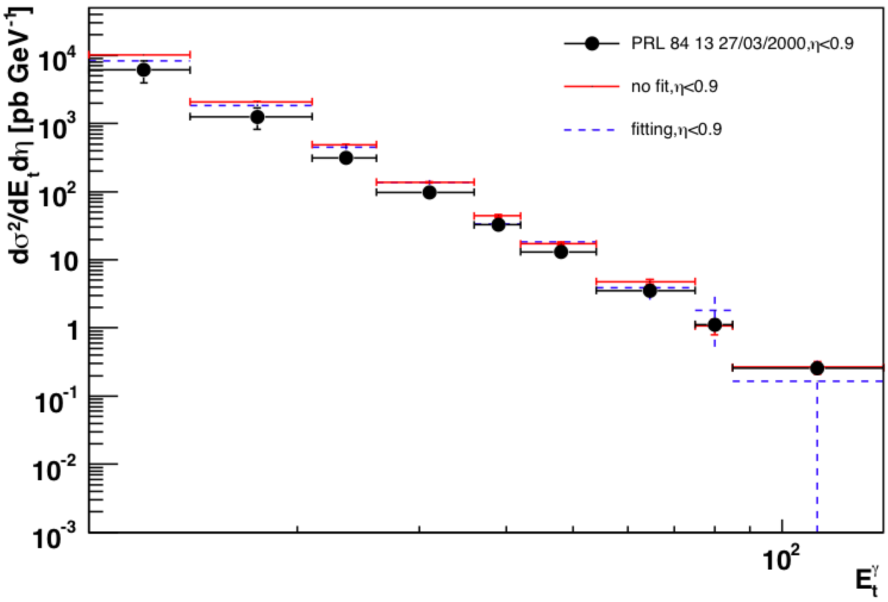

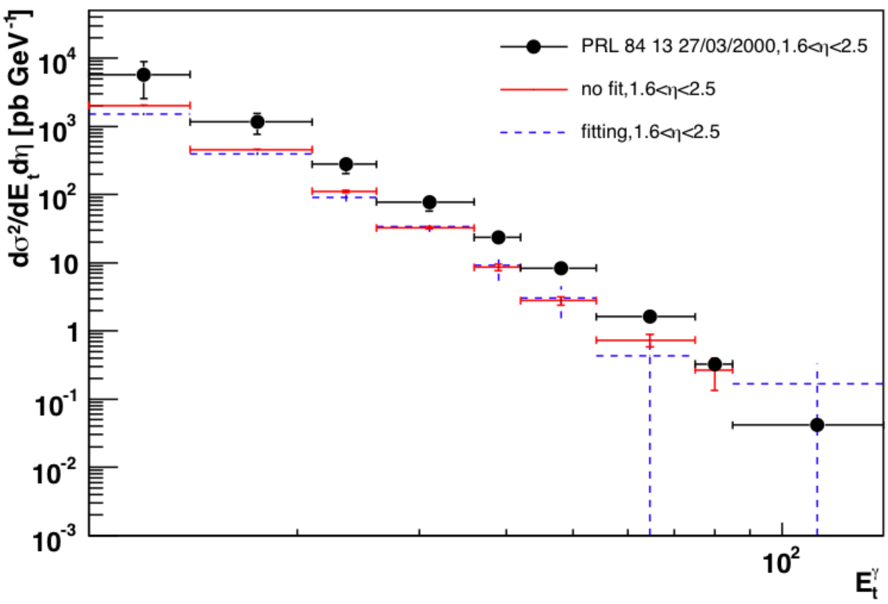

Figure 7: MC data of [3] at $\sqrt{s}$=1800 GeV, $\eta < 0.9$ (upper) and $1.6 < \eta < 2.5$ (lower), after (solid) and before (dashed) scanning

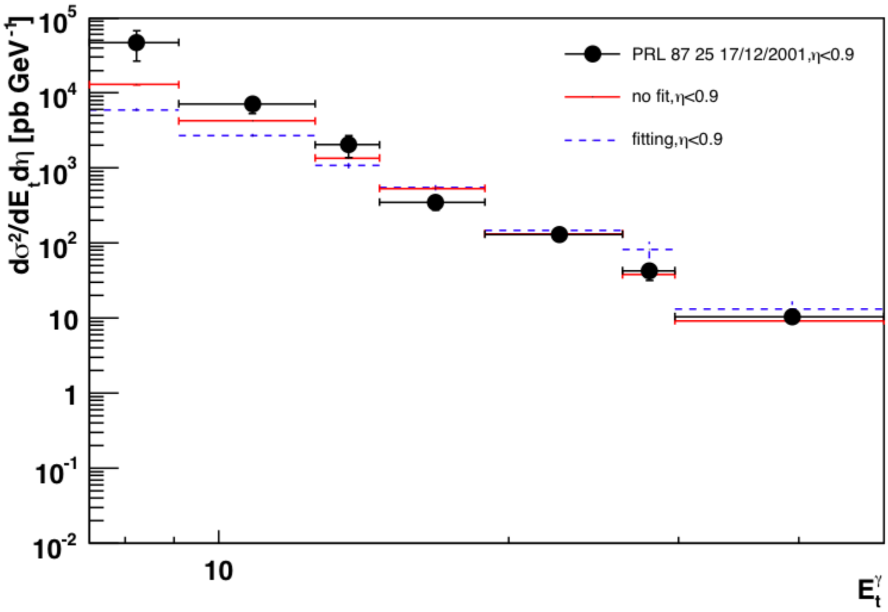

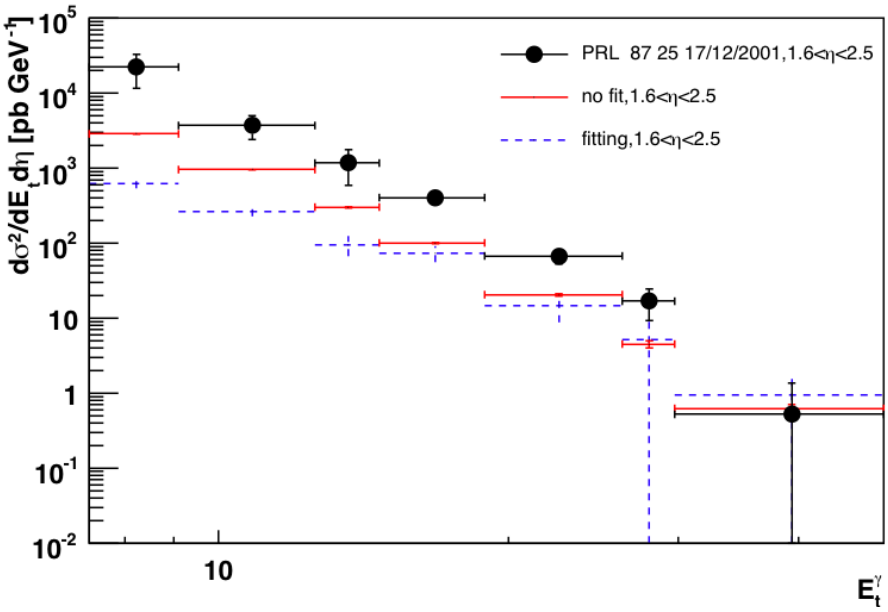

Figure 8: MC data of [4] at $\sqrt{s}$=630 GeV, $\eta < 0.9$ (upper) and $1.6 < \eta < 2.5$ (lower), after (solid) and before (dashed) scanning

A.3 Comparison of CTEQ61 with data from [2] after scanning of gluon density function

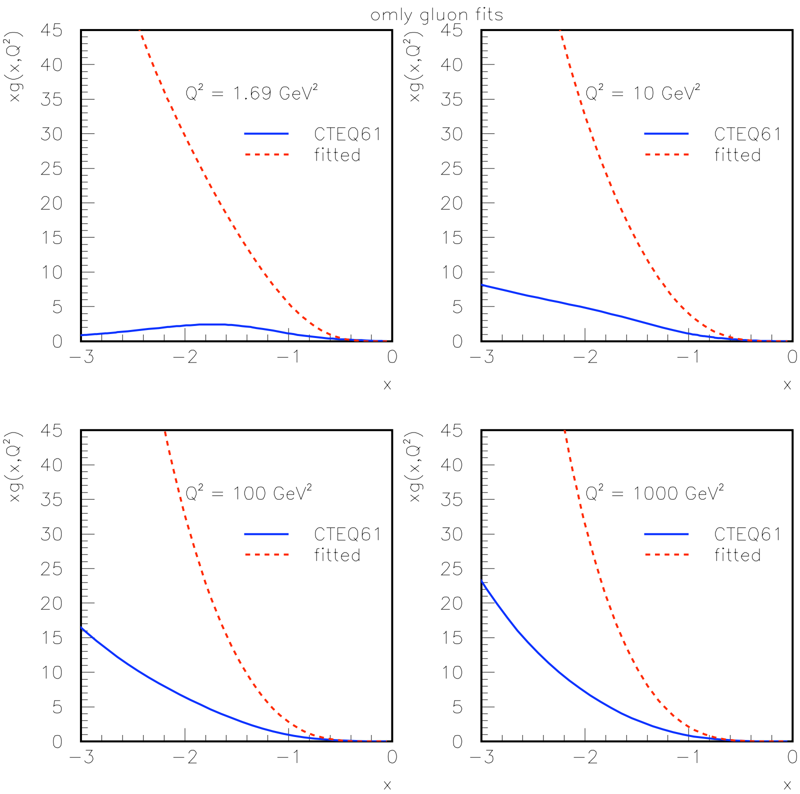

Figure 9: Gluon density function obtained from scanned data (dashed) and CTEQ61 data (solid)

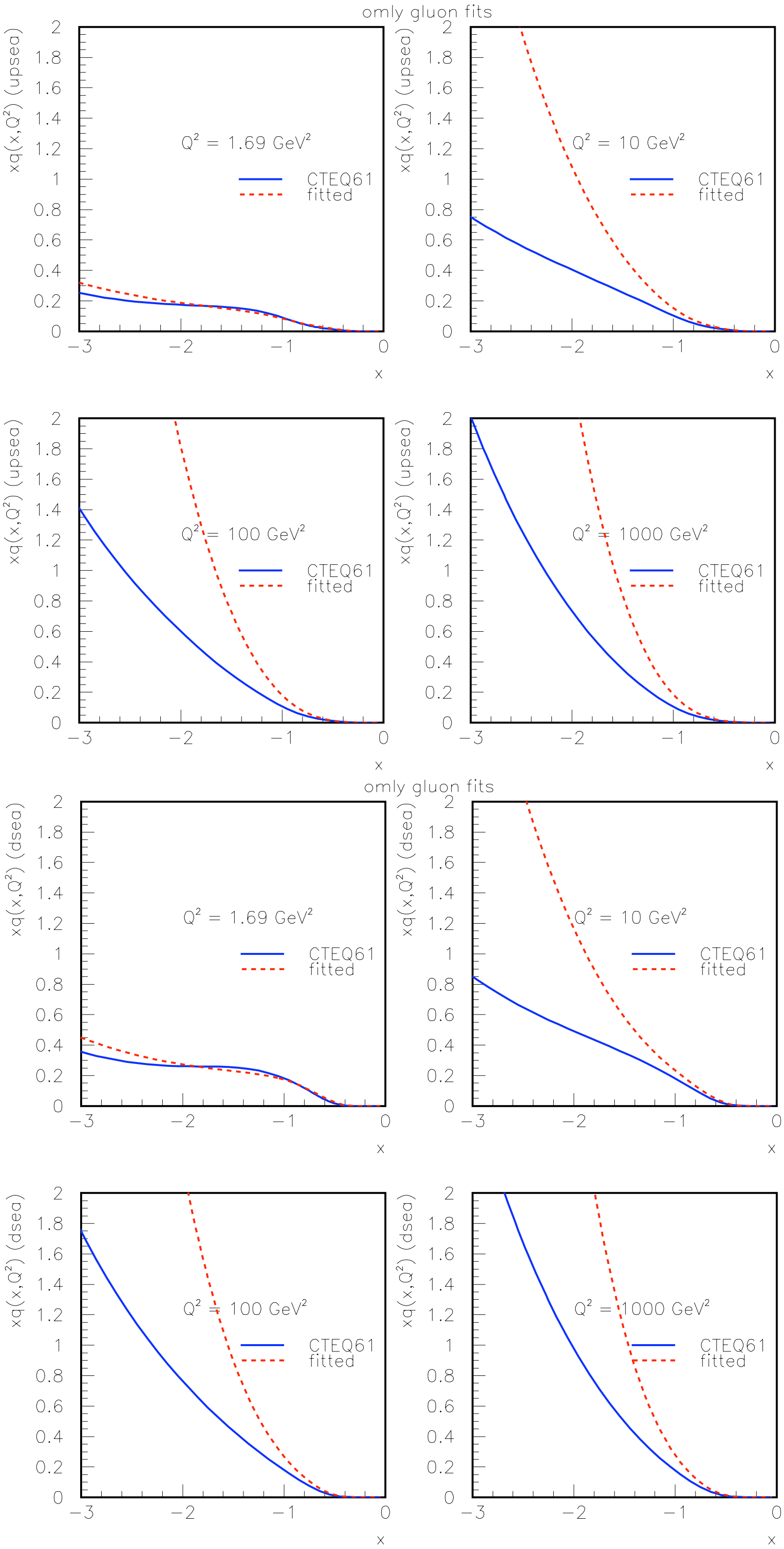

Figure 10: Sea quark density function obtained from scanned data (dashed) and CTEQ61 data (solid)

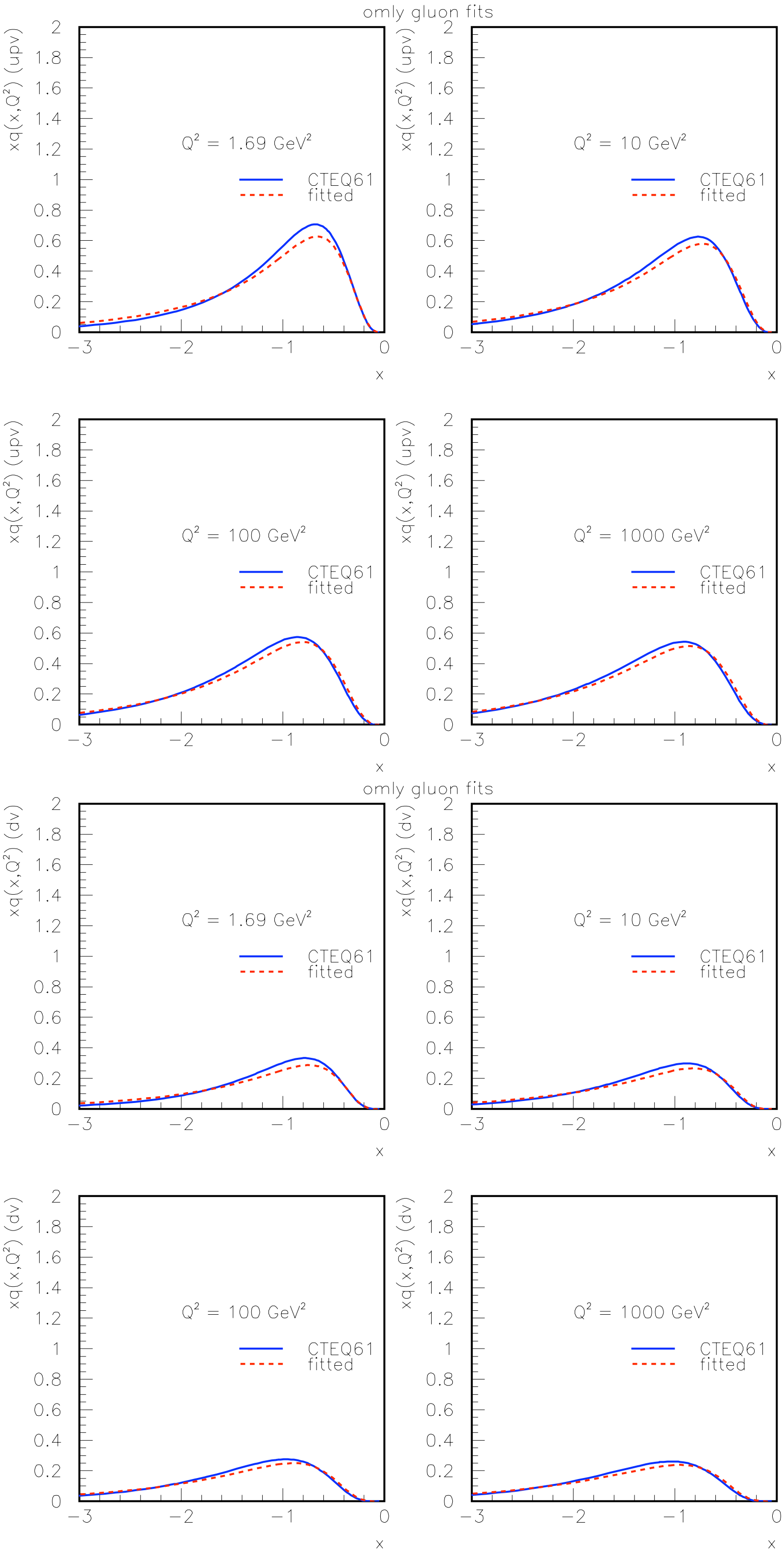

Figure 11: Valence quark density function obtained from scanned data (dashed) and CTEQ61 data (solid)

A.4 Comparison of CTEQ61 with data from [2] after scanning of gluon and quark density function

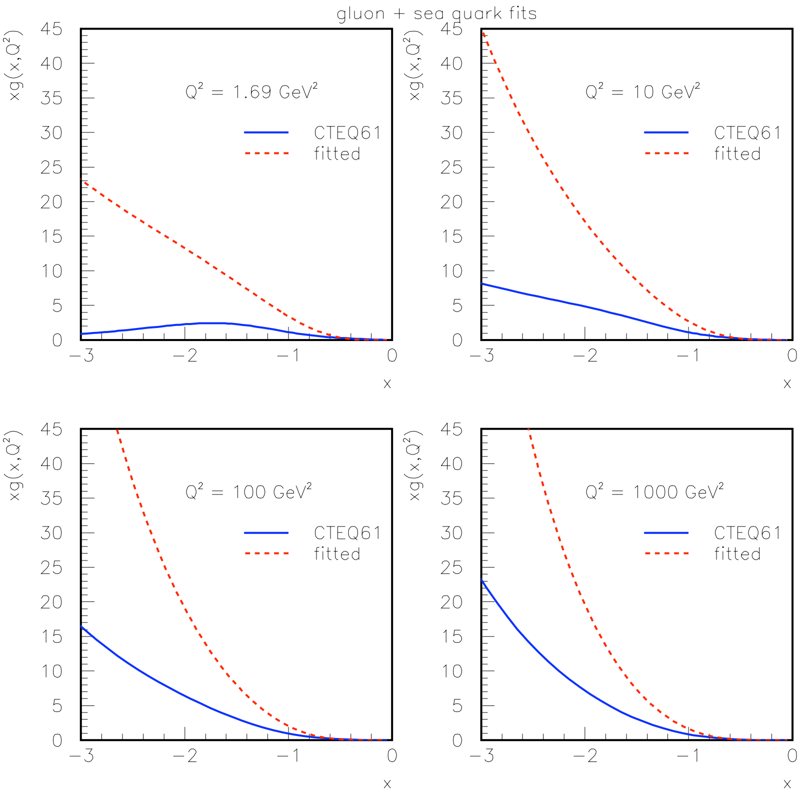

Figure 12: Gluon density function obtained from scanned data (dashed) and CTEQ61 data (solid)

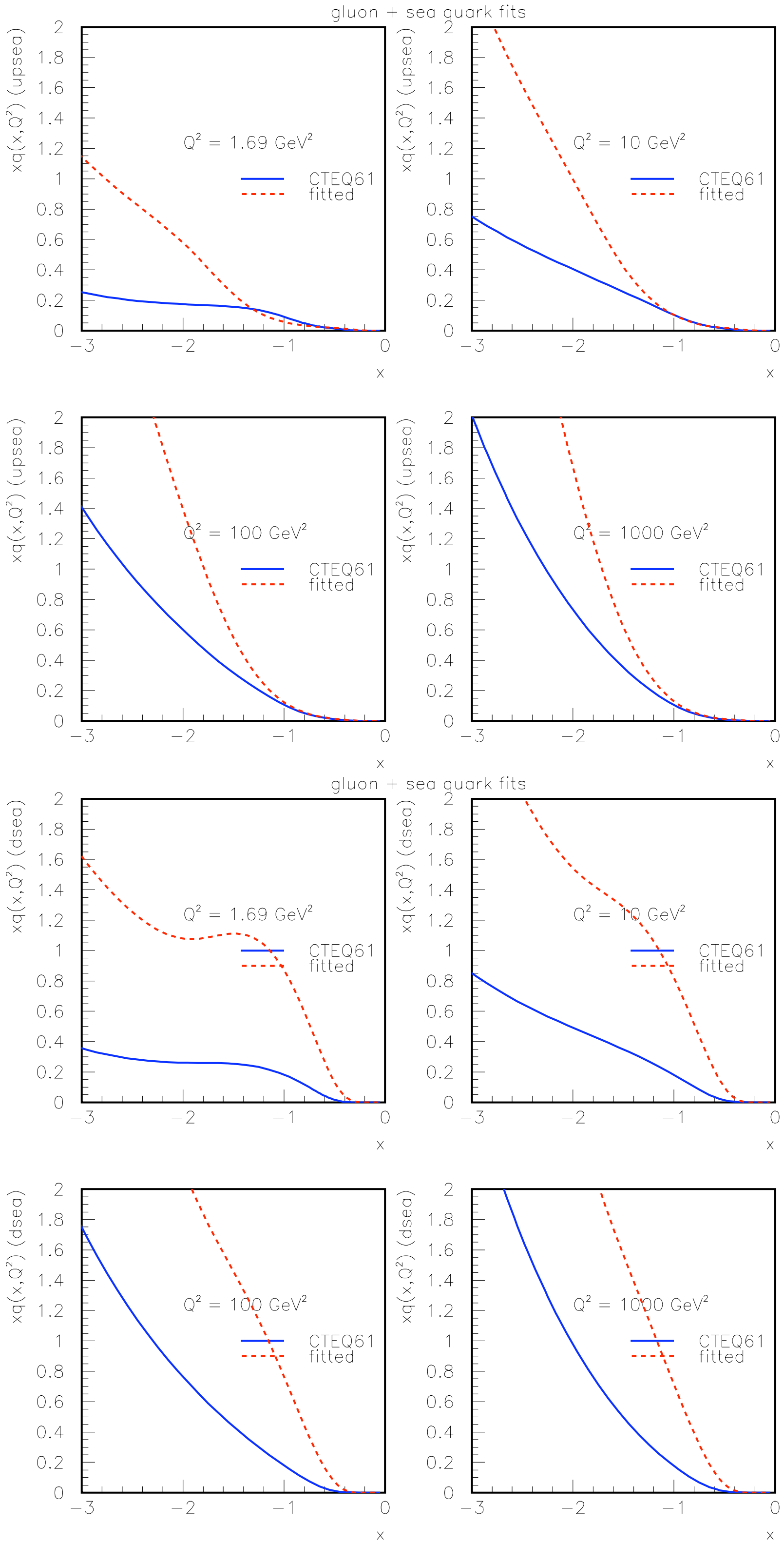

Figure 13: Sea quark density function obtained from scanned data (dashed) and CTEQ61 data (solid)

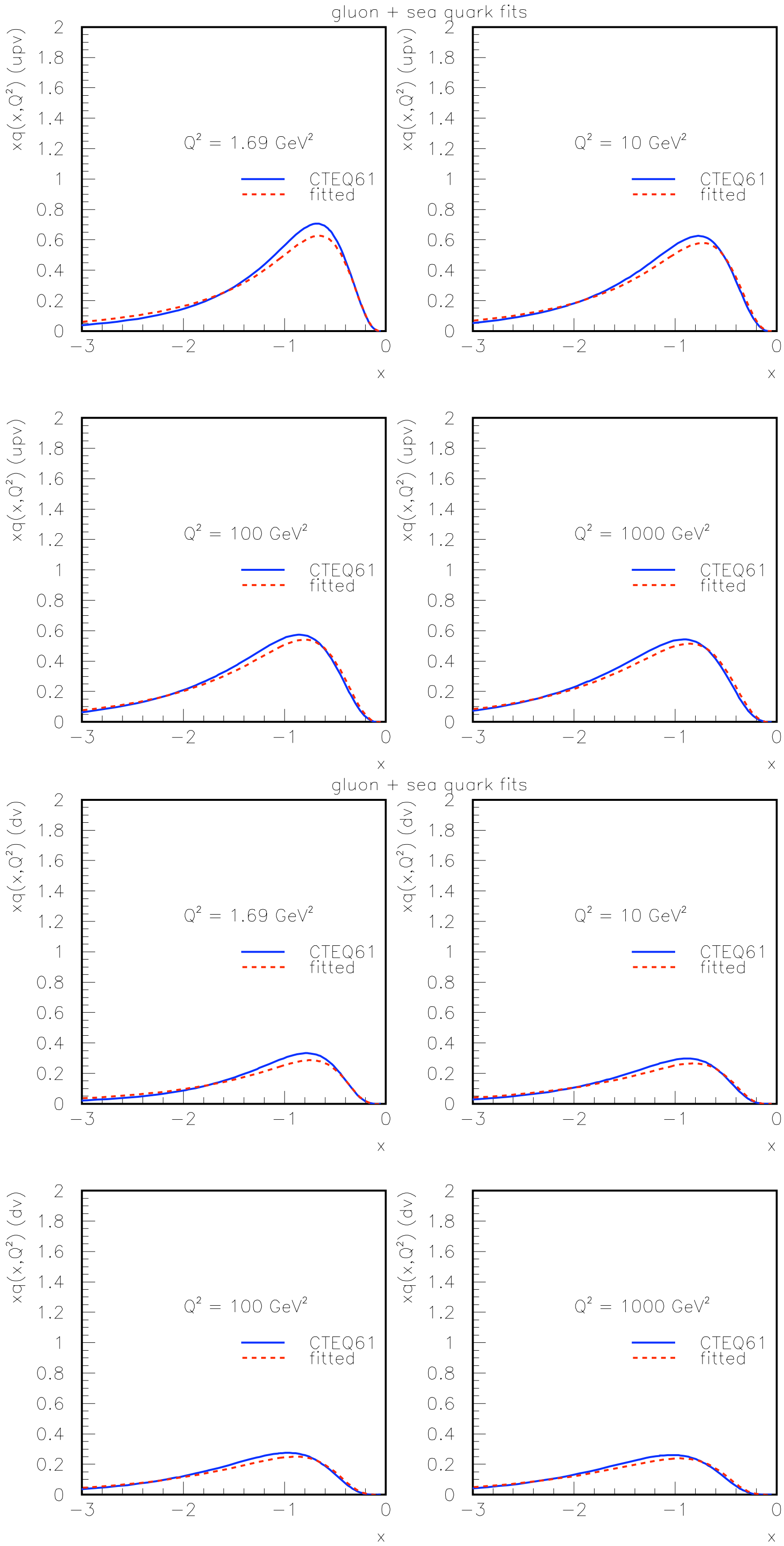

Figure 14: Valence quark density function obtained from scanned data (dashed) and CTEQ61 data (solid)

A.5 Comparison of CTEQ61 with data from [5] after scanning of gluon and quark density function

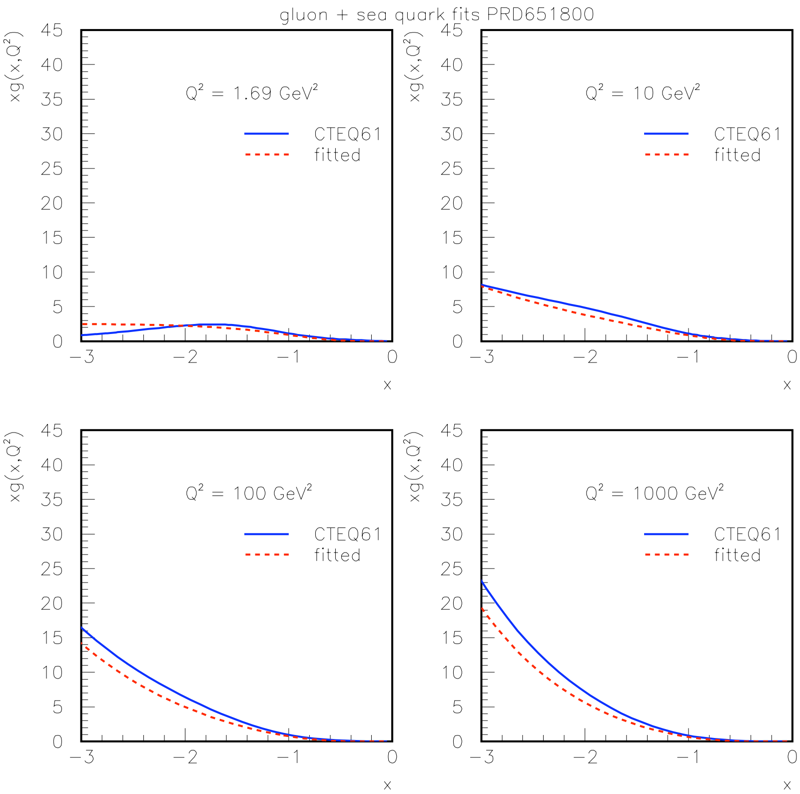

Figure 15: Gluon density function obtained from scanned data (dashed) and CTEQ61 data (solid)

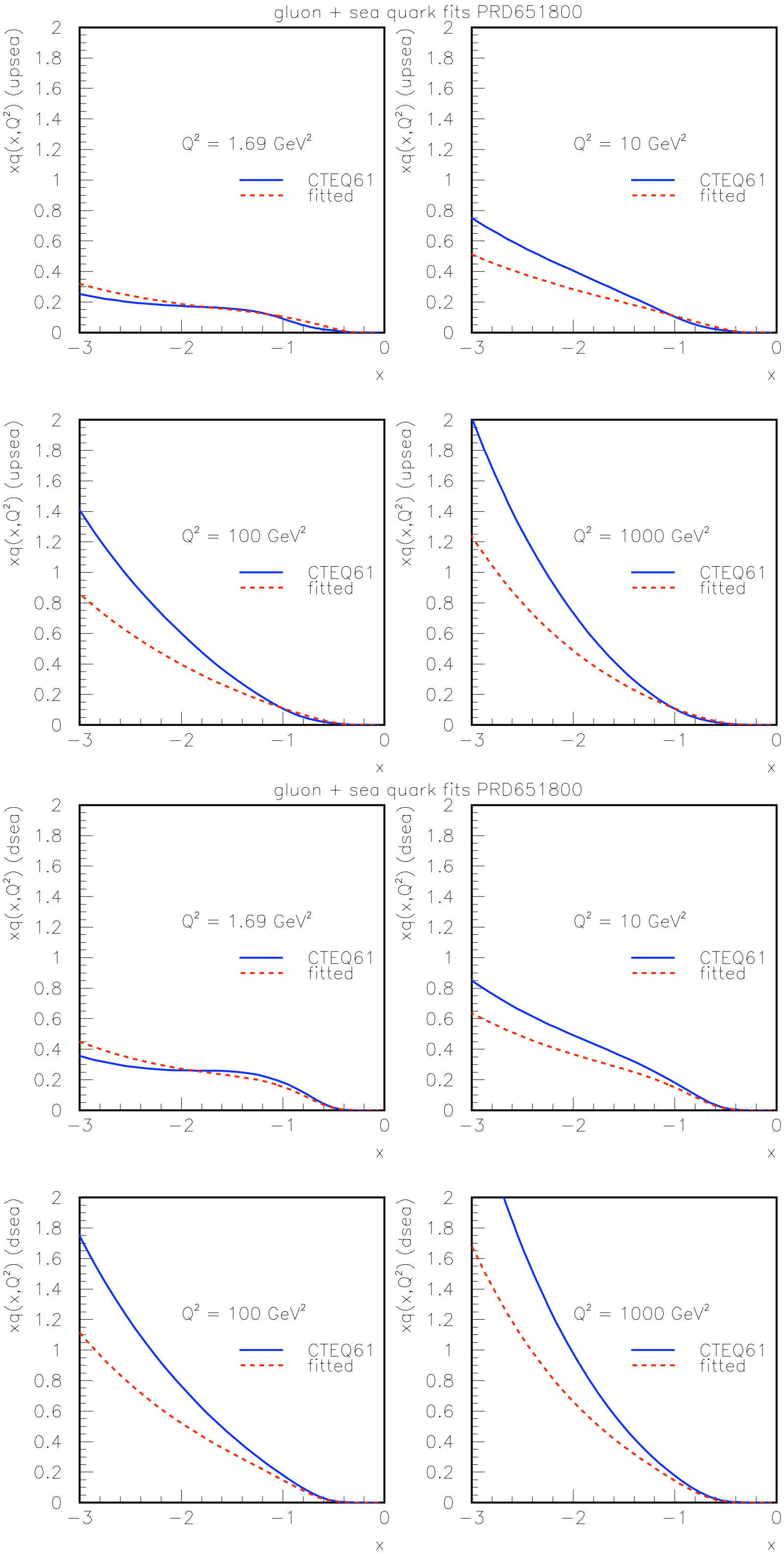

Figure 16: Sea quark density function obtained from scanned data (dashed) and CTEQ61 data (solid)

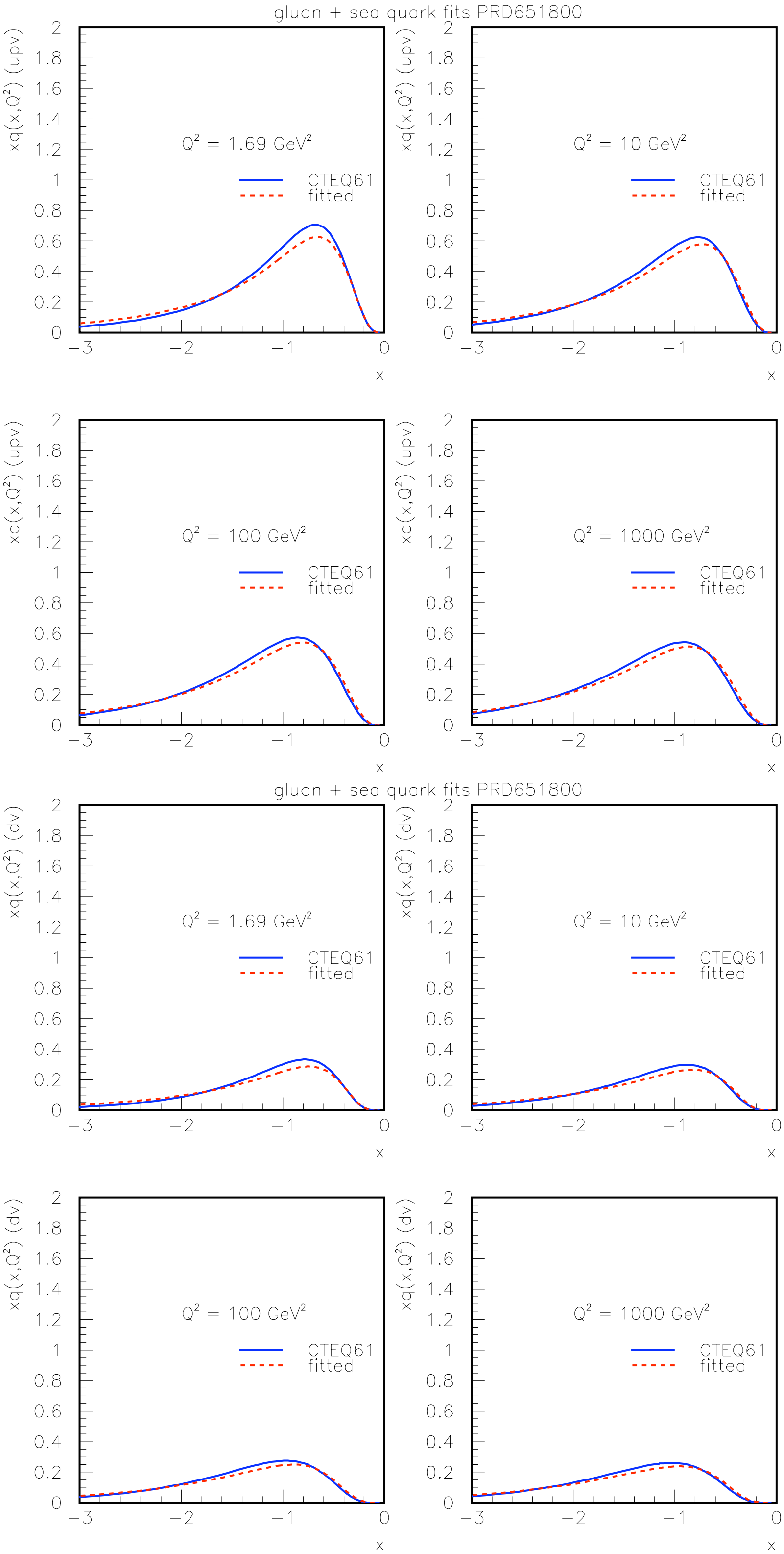

Figure 17: Valence quark density function obtained from scanned data (dashed) and CTEQ61 data (solid)